



ORIGINAL ARTICLE

Green synthesis of silver nanoparticles by seaweed endophytic *Bacillus siamensis* strain CCTB2 and their inhibitory effects against rice blast fungus

Chaiti Saha¹, Mst. Raihana Sultana¹, Fahmida Khatun¹, Efat Tara Yesmean Riya¹, Md. Abdul Kader¹, Md. Manjurul Haque², Nahid Hasan Saikat¹ and Md. Mahidul Islam Masum^{1*}

¹ Department of Plant Pathology, Gazipur Agricultural University, Gazipur 1706, Bangladesh

² Department of Environmental Science, Gazipur Agricultural University, Gazipur 1706, Bangladesh

ARTICLE INFO.

Keywords:

biosynthesis, silver nanoparticles, characterization, eco-friendly, *Pyricularia oryzae*.

Received : 7 August 2025

Revised : 20 October 2025

Accepted : 24 December 2025

Published : 05 January 2026

Citation:

Saha, C., M. R. Sultana, F. Khatun, E. T. Y. Riya, M. A. Kader, M. M. Haque, N. H. Saikat and M. M. I. Masum. 2026. Green synthesis of silver nanoparticles by seaweed endophytic *Bacillus siamensis* strain CCTB2 and their inhibitory effects against rice blast fungus. *Ann. Bangladesh Agric.* 29(2): 25-44

ABSTRACT

Pyricularia oryzae (syn. *Magnaporthe oryzae*) causes rice blast, which remains a significant threat to global rice production. Chemical fungicides are often used to manage it, but excessive use can have detrimental effects on human health and the environment. Bioinspired nanomaterials offer efficient, cost-effective, and eco-friendly alternatives to traditional methods. This study aimed to synthesize silver nanoparticles (AgNPs) using the seaweed endophytic *Bacillus siamensis* strain CCTB2 and to evaluate their antifungal effect against the rice blast pathogen *P. oryzae*. Using 16S rDNA gene sequence analysis, the endophyte bacterial isolate CCTB2, isolated from seaweed, was identified as *Bacillus siamensis* strain CCTB2. Cell-free supernatants (CFSs) from the seaweed endophytic bacterial strain CCTB2 were used to synthesize the AgNPs, which were then examined using energy-dispersive X-ray spectroscopy (EDX), electron microscopy, Fourier transform infrared spectroscopy (FTIR), and UV-visible spectroscopy. AgNP production was confirmed by the UV-visible spectra, which showed a surface plasmon resonance peak at about 430 nm. The functional groups in the CFSs of isolate CCTB2 that promoted Ag⁺ reduction, stability, and AgNPs capping were identified by FTIR spectroscopy. AgNPs have a spherical shape with an average particle size of 32.24 nm, according to electron microscopy. The presence of 2-theta emission peaks in the XRD results indicated that the biosynthesized AgNPs had a crystalline structure. The rice blast pathogen *P. oryzae* strain MP2 was significantly inhibited by biosynthesized AgNPs at 40 µg/mL, with a mycelial diameter inhibition rate of 96.65%. The mycelial morphology showed swelling and anomalies under microscopy after treatment with AgNPs. To combat rice blast fungus and preserve long-term rice productivity and food security, this study illustrated the development and use of sustainable, environmentally friendly solutions.

*Corresponding Author: Department of Plant Pathology, Gazipur Agricultural University, Gazipur 1706, Bangladesh.
Email: masum@gau.edu.bd

Introduction

Rice (*Oryza sativa* L.), a member of the Poaceae family, is the main staple crop in Bangladesh and is vital to the food security of almost 160 million people. Bangladesh produces roughly 40.7 million metric tons of rice annually, which is grown on about 28.9 million acres of land (BBS, 2024). According to Bhuiyan *et al.* (2002), almost 95% of Bangladeshis consume rice, which meets almost all their dietary protein requirements and provides 76% of their daily calories. By 2030, Bangladesh's population is anticipated to reach 223 million, requiring around 48 million tons of food grains (Bhuiyan *et al.*, 2014). However, plant diseases are a serious threat to rice production, potentially destroying enough food to feed millions of people. Several diseases significantly affect rice growth and yield, with over 70% of these caused by biological agents, including fungi, viruses, bacteria, and nematodes (Zhang *et al.*, 2009). The most harmful pathogens are fungi causing blast, sheath blight, as well as newly emerging ones like bakanae disease of rice (Raghu *et al.*, 2018; Asmaul *et al.*, 2021).

Among rice diseases, blast caused by *Pyricularia oryzae* (syn. *Magnaporthe oryzae*) is the most destructive worldwide (Wilson and Talbot, 2009). In Bangladesh, blast disease has become endemic, impacting major rice-growing regions and showing distinct race variations (Khan *et al.*, 2016; Asmaul *et al.*, 2021) is thus considered a permanent disease of rice. Rice blast manifests with four typical disease symptoms:

leaf blast, node blast, neck blast, or panicle blast (Miah *et al.*, 2013). Globally, it causes 70 to 80% rice yield loss (Nasruddin and Amin, 2013). It weakens the plant defense system without producing visible symptoms during biotrophic association and promotes cell death when it shifts to the necrotrophic association (Fernandez and Orth, 2018). While rice blast is found worldwide, the humid tropical climate of Bangladesh significantly increases infection rates by *P. oryzae*. The swift spread of rice blast disease across the nation poses a serious threat to food security, as most cultivated rice varieties are vulnerable to it. BRRI dhan28 showed the highest disease severity at 29.6%, followed by BRRI dhan29 at 25.9%, and T. Aman rice, BRRI dhan34, at 22.9%, according to Hossain *et al.* (2017). Neck blast causes the highest yield loss because it directly affects the panicle, unlike leaf blast. It is most devastating and can sometimes cause a 100% yield loss. The primary symptoms of blast disease manifest on leaves as brown spots that progress to a grey center. On the neck of the panicle, there are depressed lesions in the nodal region characterized by brown or black discolorations. Panicle blast causes a brown lesion on the grain, leading to complete degradation of the internal tissue (Kumar and Ashraf, 2019). A region characterised by elevated precipitation and a temperate climate is significantly impacted by blast disease (Ghatak *et al.*, 2013). *Pyricularia oryzae* is one of the most important plant pathogenic fungi, having an exceptional capacity to rapidly change its genetic makeup, resulting

in new pathogenic variant races (Dean *et al.*, 2012; Khan *et al.*, 2016).

The management of blast disease in rice is crucial for sustainable agriculture, primarily because the pathogen can be transmitted through seeds. Fungicidal treatment is used in rice-growing areas such as China, Vietnam, and Japan because it is economical; however, the use of synthetic pesticides increases disease resistance and creates environmental issues (Sellal *et al.*, 2021). Driven by concerns about human health and biodiversity, this movement favours the use of natural alternatives for disease control. Strategies that combine biological crop protection with ecological antagonists are being investigated, particularly in Bangladesh. Innovations like nanotechnology are becoming increasingly crucial in agriculture to address issues such as climate change and food security. Numerous studies have shown how nanoparticles improve plant germination, growth, and development (Razu and Hossain, 2015; Shang *et al.*, 2019). Compared to chemical and physical approaches, bio-inspired nanoparticles including metal nanoparticles such as silver nanoparticles offer non-toxic, stable, and environmentally acceptable ways to combat various infections (Masum *et al.*, 2019; Ali *et al.*, 2020; Saha *et al.*, 2025). While global research has shown the potential of seaweed extracts for antagonistic and bio-inspired nanoparticle (NP) synthesis, specific studies focusing on Bangladeshi seaweed resources for these applications seem limited, representing a significant research

gap and opportunity for local innovation in eco-friendly materials for agriculture and biomedical applications. In this work, biosynthesized silver nanoparticles produced by seaweed-associated endophytic bacteria were characterized, and their antibacterial efficacy against the rice blast pathogen *P. oryzae* was evaluated.

Materials and Methods

Collection of pathogen

Previously identified from an infected rice plant, the blast pathogen *P. oryzae* strain MP2 was used in this investigation (Saha *et al.*, 2025). The fungus was grown in Potato Dextrose Agar (PDA) medium containing 200g of potatoes, 20g of dextrose, and 20g of agar per liter, adjusted to pH 7.0. Following that, the culture's purity was confirmed.

Isolation of antagonistic bacteria from seaweed

In January 2024, fresh seaweed (*Gracilaria tenuistipitata* and *Sargassum oligocystum*) was acquired from the coastal areas of Bangladesh, specifically Cox's Bazar and St. Martin's Island. During collection, seaweeds were placed in a chilled container and enclosed in a sterile polybag containing saltwater, occupying more than three-quarters of the available air space. The samples were delivered to the laboratory immediately after collection. The endophytic bacteria were isolated in the Plant Pathology laboratory at GAU, Gazipur, Bangladesh.

Identification of isolated bacteria by biochemical and molecular tests

Bacterial isolates were initially identified based on their morphological, biochemical, and molecular tests. Standard tests such as Gram staining, catalase hydrolysis test, oxidase test, KOH test, gelatin liquefaction test, starch hydrolysis test, and nitrate reduction test were performed as described in Bergey's Manual of Systematic Bacteriology (Boone *et al.*, 2001).

The DNA from bacteria was extracted using the commercial DNA extraction kit (Monarch Genomic DNA purification kit). PCR for the amplification of the 16S rDNA gene from bacteria was performed using universal primers 27F (5'AGAGTTGATCCTGGCTCAG-3') as forward and 1492R (5'-GGTTACCTTGTACGACTT-3') as reverse (Masum *et al.*, 2018). PCR amplification was performed in 50 μ L total volumes with Taq 2X Master Mix with Buffers (New England Biolabs, USA) using Minicamp Thermal Cyclers (Thermo Fisher Scientific, USA). The conventional PCR reaction system (50 μ L) consisted of Taq2 X Master Mix (25 μ L), forward Primer (10 μ M) (2 μ L), reverse Primer (10 μ M): 2 μ L, DNA (2 μ L), and ddH₂O (19 μ L). The PCR results were visualized on a 1% (w/v) agarose gel, purified using a Gel extraction kit, and submitted to Biotech Concern for sequencing.

Phylogenetic analyses

Multiple sequence alignments were performed using the Clustal_X program. Phylogenetic

trees were generated using the neighbor-joining method in the MEGA 11.0 program. Bootstrap replication (1000) was used to analyze the nodes in the phylogenetic trees.

Preparation of the cell-free supernatants (CFSs) of the endophytic bacterium

The cell-free supernatants (CFSs) of the selected endophytic bacterium isolated from seaweed were prepared according to Masum *et al.* (2018) with slight modifications. In brief, the isolated bacteria were inoculated in freshly prepared nutrient broth and incubated at 30 °C and 200 rpm for 2 days. The bacterial culture (about $\sim 1 \times 10^8$ CFU/mL) was centrifuged twice at 10,000 rpm, 4 °C for 20 minutes, and 0.22 μ m filter was used to purify the CFSs. A 100 μ L of CFSs was spread out on NA media for a day to rule out any potential contamination. The CFSs were kept at 4 °C till their use in the biosynthesis of AgNPs.

Biosynthesis of silver nanoparticles (AgNPs)

The CFSs were used for the biosynthesis of AgNPs according to the procedure described by Ibrahim *et al.* (2020). Briefly, 10 mL of CFSs were mixed with 90 mL of an aqueous AgNO₃ solution (2 mM) in a 250 mL Erlenmeyer flask. After that, the mixture was incubated in the dark for three days at 30 °C and 200 rpm on a rotary shaker. As a control, 10 mL of NA broth containing the same amount of AgNO₃ was used. They were periodically checked for a visible color change from yellow light to dark brown, indicating the formation of silver nanoparticles, which were further confirmed

by UV spectrophotometry. After successful nanoparticle synthesis, the pellets were collected by centrifugation, freeze-dried, and stored at -80°C for further characterization.

Characterization of AgNPs mediated by CCTB2 bacteria

UV-vis spectrophotometry and Fourier transform-infrared spectroscopy (FTIR)

The biosynthesis of AgNPs, resulting from the reduction of silver metal ions using CFSs of *Bacillus siamensis* strain CCTB2, was monitored using a UV-2550 Shimadzu Spectrophotometer (Shimadzu Corporation, Kyoto, Japan) with a resolution of 1 nm and a wavelength range of 200-800 nm. To identify the functional groups responsible for the stabilization and capping of the biosynthesized AgNPs, Fourier-transform infrared (FTIR) spectroscopy of the freeze-dried nanoparticles was performed in the spectral range of 4000–500 cm^{-1} (Singh *et.al.*, 2016).

TEM observation and EDX spectrum analysis

The morphology of the biosynthesized AgNPs was determined according to the method of using Transmission Electron Microscopy (TEM) (JEM-1230, JEOL, Akishima, Japan). In brief, the sample was prepared with a copper-coated grid for 24 h at room temperature to make a film of the AgNPs sample. The excess liquid was discarded and kept in a grid box sequentially. The EDX (energy-dispersive X-ray) spectrum was performed to examine

the metallic nature, elemental compositions, and purity of synthesized AgNPs using the detector attached to FE-TEM (Singh *et.al.*, 2016).

X-ray diffraction (XRD) analysis

The XRD patterns of the biosynthesized AgNPs were analyzed as described by Fouad *et al.* (2014) using an Xpert PRO diffractometer (Holland) with a detector voltage of 45kV and a current of 40mA using Cu $\text{K}\alpha$ radiation. The recorded range of 2θ was 0–80° with a scanning speed of 6° min $^{-1}$.

Antifungal activity of the biosynthesized AgNPs against *P. oryzae*

Effect of AgNPs on mycelium growth

The inhibitory effect of AgNPs at three concentrations (20, 30, and 40 $\mu\text{g/mL}$) on mycelium growth of *P. oryzae* strain was determined using a potato dextrose agar (PDA) medium as described by Ibrahim *et al.* (2020) with slight modification. In brief, a disk of 7-day-old mycelium (10 mm in diameter) was introduced into the center of petri dishes (9 cm in diameter) containing Potato Dextrose Agar (PDA) medium (pH 7.0) supplemented with various concentrations of AgNPs. The PDA plates were used as a control without AgNPs. The diameter of the fungal colony was assessed after 7 days of incubation at 27 °C, followed by the calculation of mycelial growth inhibition. The inhibition rate was calculated using the following equation.

$$\text{Rate of Inhibition (\%)} = \frac{R-r}{R} \times 100$$

where 'R' represents the radial growth of fungal mycelium in control plates, and 'r' is the radial growth of fungal mycelium in AgNPs-treated plates (Hari *et al.*, 2023). This assay was performed with a minimum of three independent replicates, incorporating suitable controls in each experiment and maintaining consistent experimental conditions across all replicates to ensure the accuracy and reliability of the results.

Effect of AgNPs on cell wall morphology

Damage to the cell wall of *P. oryzae* strain MP2 was assessed using AgNPs according to the method of Gao *et al.* (2016), with minor modifications. Briefly, a mycelial disc of *P. oryzae* strain MP2 (10 mm in diameter) was taken from PDA medium, treated and untreated with AgNPs, and examined under a compound microscope in the plant pathology laboratory at GAU.

Statistical analysis

All experiments were conducted using a completely randomized design. Data were subjected to an analysis of variance (ANOVA) test using Statistix 10 (Analytical Software). The data presented were from representative experiments repeated at least twice with similar results. Individual comparisons of mean values were conducted using the least significant difference (LSD) test ($P<0.05$).

Results and Discussions

Isolation of the seaweed endophytic bacteria

A total of nine endophytic bacteria were isolated from two seaweed species. Of these,

seven isolates originated from the seaweed species *Gracilaria tenuistipitata* (CCTB1, CCTB2, CCTB3, CCTB4, CCTB5, CCTB6, and CCTB7), while two isolates (SD1 and SD2) were obtained from *Sargassum oligocystum*. Among all isolates, only CCTB2 demonstrated the unique ability to biosynthesize silver nanoparticles (AgNPs), as confirmed by UV-visible spectrophotometry. This isolate was subsequently identified and characterized (Fig. 1-3). Several studies also reported that marine algal species harbor diverse microorganisms, particularly fungal and bacterial endophytes, which may be utilized in biological control (Juhmani *et al.*, 2020; Suji *et al.*, 2024). Endophytes in algal tissues are explored as sources of novel natural products and biocontrol agents, with a focus on isolating their abilities to combat plant pathogens and synthesize nanoparticles. Bangladesh possesses extensive coastal and marine biodiversity, particularly along the Bay of Bengal, where diverse marine macroalgae are abundant yet underutilized. Utilizing indigenous seaweed species for eco-friendly nanoparticle synthesis offers biodegradable and non-toxic alternatives to traditional chemical methods.

Phylogenetic identification of isolate CCTB2 based on the sequences of 16S rDNA

The 16S rDNA gene sequence of endophytic bacterial isolate CCTB2 was successfully amplified using a universal 16S primer, confirming the product size of approximately

1.5 kb (Fig. 2a). The NCBI Blast homology analysis revealed high similarity values (98.46–98.53%), indicating that the 16S rDNA sequence of the endophytic isolate CCTB2 was nearly identical to several *Bacillus* type strains, including *Bacillus siamensis* KCTC 13613, *Bacillus subtilis* subsp. *subtilis* str. 168, *Bacillus subtilis* subsp. *subtilis* NBRC 13719, and *Bacillus velezensis* strain NRRL B-41580 (Fig. 1). The sequences were also analyzed to justify further using the EzBioCloud database (<https://www.ezbiocloud.net/>). A phylogenetic tree constructed from 16S rDNA data indicated that isolate CCTB2 was closely related to *Bacillus siamensis* KCTC 13613 (MN176482.1), forming the same clade with a bootstrap value of 58, while being distinctly separated from the type strains of other species of the same family, such as *B. subtilis* subsp. *subtilis*, *B. velezensis*, *B. amyloliquefaciens*, *B. nematocidal*, *B. inaquosorum*, *B. tequilensis*, *B. stercoris* etc. To construct the neighbouring-joining tree, the type strain *Bacillus cereus* ATCC 14579

(NR 074540.1) was used as an outgroup. The findings indicated that the strain CCTB2 is classified within *B. siamensis*. The 16S rDNA gene sequence of strain CCTB2 has been submitted to GenBank under accession number PX580557. In accordance with this work, phylogenetic identification of bacteria was frequently performed in other research by analyzing the nucleotide sequences of the 16S ribosomal DNA (rDNA) gene, a conventional molecular technique for describing and classifying microbial communities (Masum *et al.*, 2018; Mahajan *et al.*, 2025). Researchers demonstrated that seaweed endophytic bacterial communities were highly diverse and primarily comprised specific genera, particularly those belonging to the Firmicutes, including *Bacillus* (Masum *et al.*, 2018; Ibrahim *et al.*, 2020).

*Morphological, physiological, and biochemical characterization of *B. siamensis* strain CCTB2*

The strain CCTB2 was rod-shaped, producing fast-growing, rounded to irregular, elevated, smooth-surfaced colonies. Moreover, it

	Description	Scientific Name	Max Score	Total Score	Query Cover	E value	Per. Ident	Acc. Len	Accession
<input checked="" type="checkbox"/>	<i>Bacillus siamensis</i> KCTC 13613 16S ribosomal RNA gene, partial sequence	<i>Bacillus siamens...</i>	2519	2519	100%	0.0	98.53%	1473	MN176482.1
<input checked="" type="checkbox"/>	<i>Bacillus subtilis</i> subsp. <i>subtilis</i> str. 168 genome assembly, chromosome: 1	<i>Bacillus subtilis...</i>	2514	24937	100%	0.0	98.46%	4215606	AL009126.3
<input checked="" type="checkbox"/>	<i>Bacillus subtilis</i> subsp. <i>subtilis</i> 6051-HGW, complete genome	<i>Bacillus subtilis...</i>	2514	24937	100%	0.0	98.46%	4215610	CP003329.1
<input checked="" type="checkbox"/>	<i>Bacillus subtilis</i> subsp. <i>subtilis</i> str. 168 chromosome	<i>Bacillus subtilis...</i>	2514	24528	100%	0.0	98.46%	4215385	CP019663.1
<input checked="" type="checkbox"/>	<i>Bacillus subtilis</i> subsp. <i>subtilis</i> NBRC 13719 DNA, complete genome	<i>Bacillus subtilis...</i>	2514	25011	100%	0.0	98.46%	4211090	AP019714.1
<input checked="" type="checkbox"/>	<i>Bacillus subtilis</i> strain NCIB_3610 chromosome, complete genome	<i>Bacillus subtilis...</i>	2514	25000	100%	0.0	98.46%	4215634	CP130597.1
<input checked="" type="checkbox"/>	<i>Bacillus subtilis</i> subsp. <i>subtilis</i> strain DSM 10 chromosome, complete genome	<i>Bacillus subtilis...</i>	2514	25000	100%	0.0	98.46%	4215636	CP060710.1
<input checked="" type="checkbox"/>	<i>Bacillus velezensis</i> strain NRRL B-41580 16S ribosomal RNA gene, partial sequence	<i>Bacillus velezensis</i>	2514	2514	100%	0.0	98.46%	1508	KY694464.1

Fig. 1. BLAST search analysis based on 16S rDNA gene sequence of isolate CCTB2.

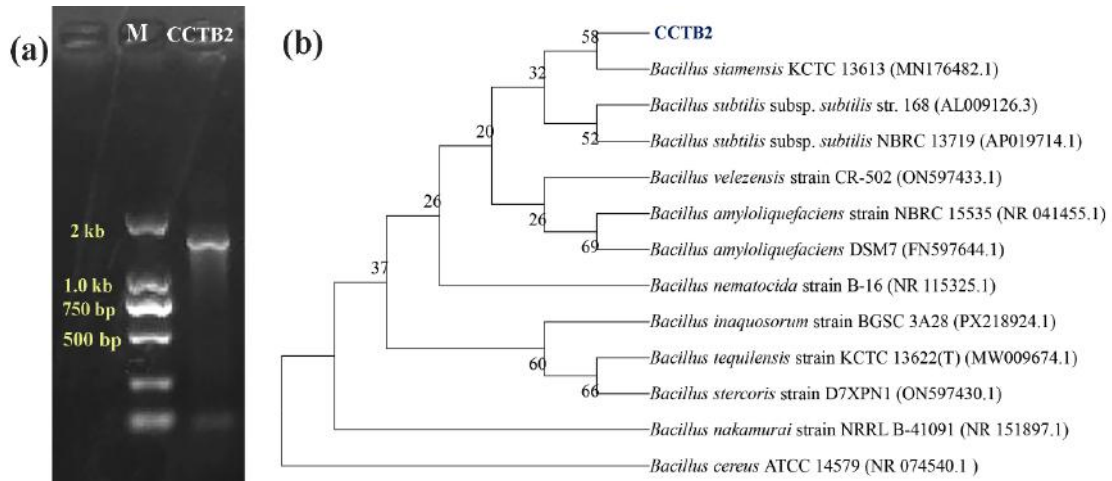


Fig. 2. Molecular identification of seaweed endophytic bacteria isolate CCTB2. (a) Validation of 16S rDNA genes for the isolate CCTB2 endophytic bacteria, M: Marker DL2000; (b) A phylogenetic tree of endophytic bacteria using the Neighbor-Joining method based on 16S rDNA gene sequence analysis. The bootstrap consensus tree was inferred from 1000 replicates. The type material, *Bacillus cereus* ATCC 14579, was used as the outgroup.

produced sticky, wet colonies on LB agar medium (Fig. 4a). The tested isolate exhibited positive results for Gram staining, KOH solubility, catalase test, oxidase test, nitrate reduction test, gelatin liquefaction test, and indole production test, while demonstrating a negative reaction in starch hydrolysis (Fig. 3). Earlier studies reported that *Bacillus* spp. were shown to be positive for Gram staining, catalase, oxidase, and nitrate reduction tests (Rajashekhar *et al.*, 2017), which is consistent with the present work. Consequently, biochemical tests from other investigations corroborated our findings, affirming the bacterium as *Bacillus* sp. Similar to our results, the genus *Bacillus* showed a negative result in the starch hydrolysis test (Joseph *et al.*, 2018) and a positive result in the gelatin liquefaction test (Sarode *et al.*, 2019).

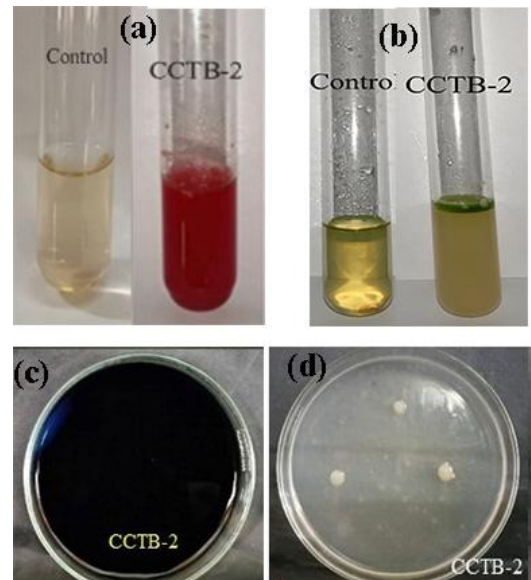


Fig. 3. Biochemical tests of seaweed endophytic bacterial isolate CCTB2. (a) Nitrate test; (b) Indole test; (c) starch hydrolysis test; (d) Gelatin liquefaction test

Biosynthesis of AgNPs mediated by *B. siamensis* strain CCTB2

The endophytic bacterial isolate CCTB2, obtained from seaweed *Gracilaria tenuistipitata*, was used to synthesize silver nanoparticles (AgNPs). The cell-free culture filtrate of *B. siamensis* strain CCTB2 caused a color change from light yellowish to dark brown, indicating the complete reduction of Ag^+ to Ag^0 within two days (Fig. 4a). Additionally, a UV-Vis spectrophotometer

was used to confirm nanoparticle production. The SPR spectra of AgNPs in the cell-free culture filtrate of strain CCTB2 showed a sharper and stronger absorption band at 430 nm (Fig. 4b). Subsequently, the nanoparticles were freeze-dried for further analysis. Consistent with this study, earlier research reported that UV absorption peaks of AgNPs ranged from 400 to 450 nm, with observations at 420, 430, and 480 nm in various experiments (Manikandan *et al.*, 2017; Hossain *et al.*, 2023; Saha *et al.*, 2025).

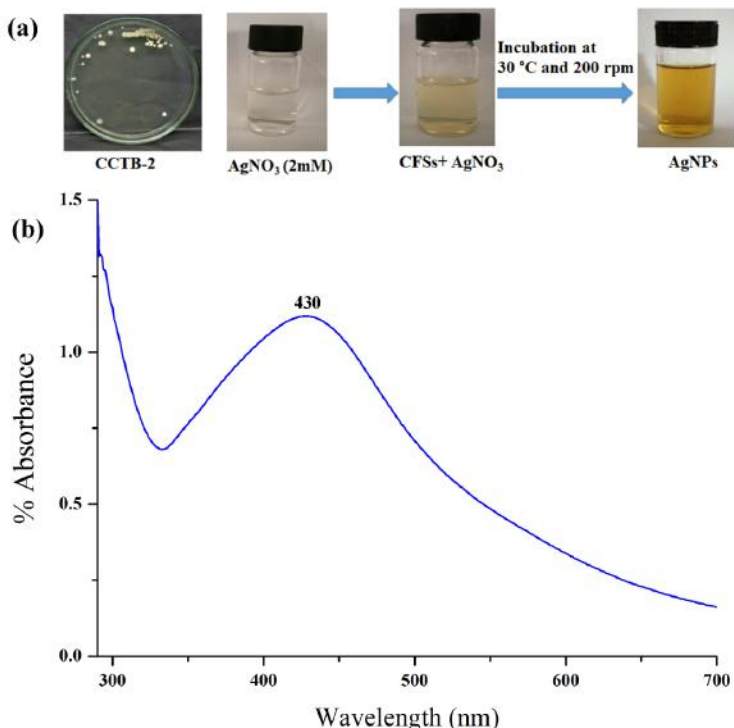


Fig. 4. Confirmation of the ability of cell-free culture filtrate (CFCs) of *B. siamensis* strain CCTB2 to biosynthesize silver nanoparticles (AgNPs). (a) Schematic diagram of the biosynthesis of AgNPs mediated by CFCs of *B. siamensis* strain CCTB2; (b) UV-Vis spectra of AgNPs biosynthesized using CFCs of *B. siamensis* strain CCTB2. The peak at 430 nm corresponds to the surface plasmon resonance of the AgNPs.

Indigenous seaweed species and the bacteria that live with them could be good alternatives to making chemical nanoparticles. They could be useful for healthcare (as antimicrobial and anticancer medicines), agriculture (plant disease management and nano-fertilizers), and environmental remediation.

Characterization of biosynthesized AgNPs

Fourier-transform infrared (FTIR) spectroscopy was employed to identify the functional biomolecules involved in the capping and stabilisation of the silver nanoparticles. The FTIR spectrum of silver nanoparticles (AgNPs) derived from the CFC of bacterial isolate CCTB2 is depicted in Fig. 5. There was a total of 8 bands detected at the following wavelengths for AgNPs mediated

by bacterial isolate CCTB2: 3271.46, 2919.20, 2844.48, 2262.71, 1619.57, 1371.39, 1032.47, 637.51 as derived from several research studies (Fig. 5 & Table 1). FTIR spectroscopy analysis identified specific functional groups in the CFCs of *B. siamensis* strain CCTB2 that facilitated the reduction of Ag⁺, stabilization, and the capping of AgNPs.

The peaks identified in the spectrum of AgNPs synthesized using CFCs of bacterial isolate CCTB2 are summarized in Table 1. The significant FTIR peaks corresponding to O–H stretching vibrations, C–H stretching, C=O stretching, C–H bending, C–H stretching in CH₃, C–O stretching, and C–N stretching vibrations demonstrated the presence of

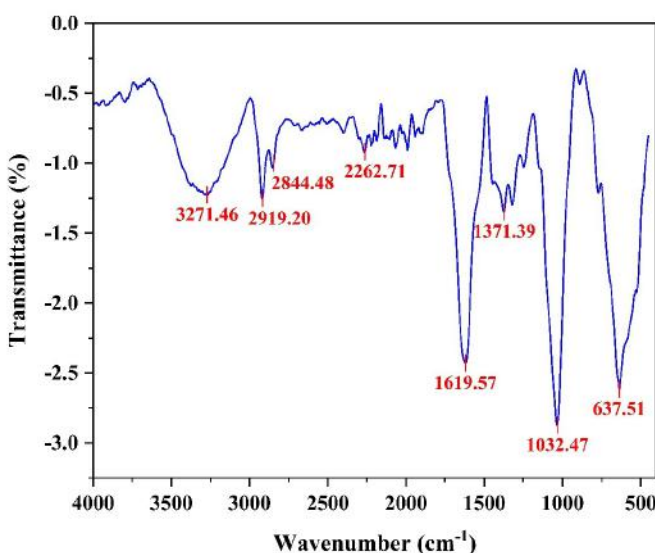


Fig. 5. Fourier transform infrared (FTIR) spectra of biosynthesized (AgNPs) from CFC of *Bacillus siamensis* isolate CCTB2 displaying functional groups accountable for the AgNPs synthesis and their stabilization.

potential functional groups, suggesting their involvement in the stabilization and capping of AgNPs (Jyoti *et al.*, 2016; Dada *et al.*, 2017; Chafidz *et al.*, 2020; Huq, 2020; Tiwari *et al.*, 2023; Saha *et al.*, 2025).

The silver nanoparticles (AgNPs) produced using the bacterial isolate CCTB2 were further examined by XRD and TEM. The XRD test results demonstrated that the biosynthesized AgNPs exhibited a crystalline structure, as indicated by the presence of 2-theta emission peaks. The X-ray diffraction pattern of the AgNPs exhibited characteristic Bragg reflection peaks at 2-theta values of 38.200, 44.400, 64.600, 77.5970, and 88.755°. These peaks correspond to the silver crystal planes (111), (200), (220), (311), and (322), respectively, as illustrated in Fig. 6. The observation of these reflection peaks is linked to the crystallographic properties of the centring face and the cubic structure of AgNPs. The X-ray diffraction pattern was

obtained using the JCPDS standard powder diffraction card, specifically the silver file No. 06-0480. The observed pattern provided evidence that the particles produced during biosynthesis were indeed silver nanoparticles. The results of this study are in line with those obtained from another research (Manikandan *et al.*, 2017; Fouda *et al.*, 2020; Hossain *et al.*, 2023)

The characteristics of the produced AgNPs, including size, shape, and morphology, were analysed using Transmission Electron Microscopy (TEM). The morphology of silver nanoparticles (AgNPs) was predominantly spherical. The dimensions of AgNPs mediated by CCTB2 ranged from 20 to 50 nm, with an average size of 32.24 nm (Fig. 7). The variations in particle size observed between transmission electron microscopy (TEM) and in situ dynamic light scattering techniques can be attributed to aggregation that occurs during the sample

Table 1. Relation of the prominent peaks found in FTIR spectra of the biosynthesized AgNPs using *Bacillus* sp. isolate CCTB2

Peak	Bands	Possible functional group	Compound Class	References
1	3271.46	stretching vibration of O-H groups	aromatic ring	Huq, 2020
2	2919.20	C–H stretching	alkanes	Chafidz <i>et al.</i> , 2020
3	2844.48	C–H stretching	alkane	Huq, 2020
4	2262.71	C–H stretch	aldehydes	Dada <i>et al.</i> , 2017
5	1619.57	The C = O stretching	amide or vinylic keto	Tiwari <i>et al.</i> , 2023
6	1371.39	C–H stretching in CH ₃ , C–O stretching, CH bending	aliphatic	Darweesh <i>et al.</i> , 2022
7	1032.47	C–N stretch vibration	amines	Jyoti <i>et al.</i> , 2016
8	637.51	C–H bending	alkyne	Dada <i>et al.</i> , 2017

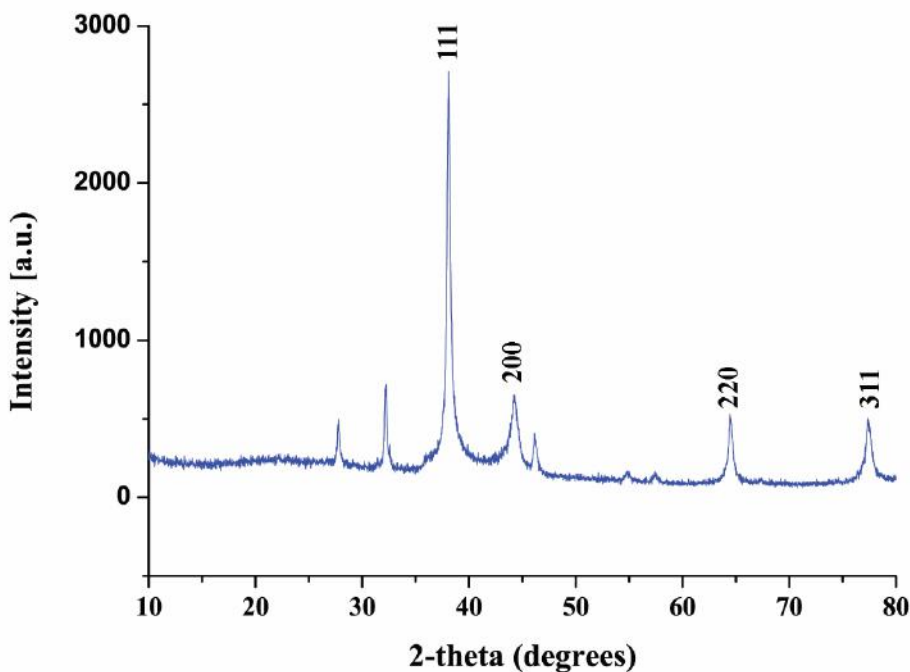


Fig. 6. X-ray diffraction spectrum demonstrating the nanosize and crystalline nature of the AgNPs mediated by *Bacillus siamensis* strain CCTB2.

preparation process (Liu and Hurt, 2010). Similarly, Sun *et al.* (2014) documented that TEM images of AgNPs produced using a 5% (v/v) diluted tea extract (1 g/L TOC) revealed an AgNPs size distribution spanning from 20 to 90 nm. Additionally, energy dispersive spectroscopy validated that metal silver (Ag^0) predominated in the synthesized AgNPs (Fig. 8). The characteristic absorption peak of the Ag element was observed in AgNPs at 3 KeV, confirming that pure silver existed at the nanoscale, as previously reported (Masum *et al.*, 2019; Ibrahim *et al.*, 2020; Hossain *et al.*, 2023; Saha *et al.*, 2025). In agreement with

the EDX of AgNPs in another investigation, the EDS spectrum indicated seven different peaks, of which oxygen (6.08%), carbon (60.34%), and silver (15.2%) were detected (Fig. 8). These findings were consistent with the findings of the EDS spectrum (Saha *et al.*, 2025).

In vitro antimicrobial activity of AgNPs

The antifungal activity analysis revealed that AgNPs produced from *B. siamensis* strain CCTB2 effectively inhibited the mycelial growth of *P. oryzae* isolate MP-2, as depicted in Fig. 9. The inhibitory effect of AgNPs on

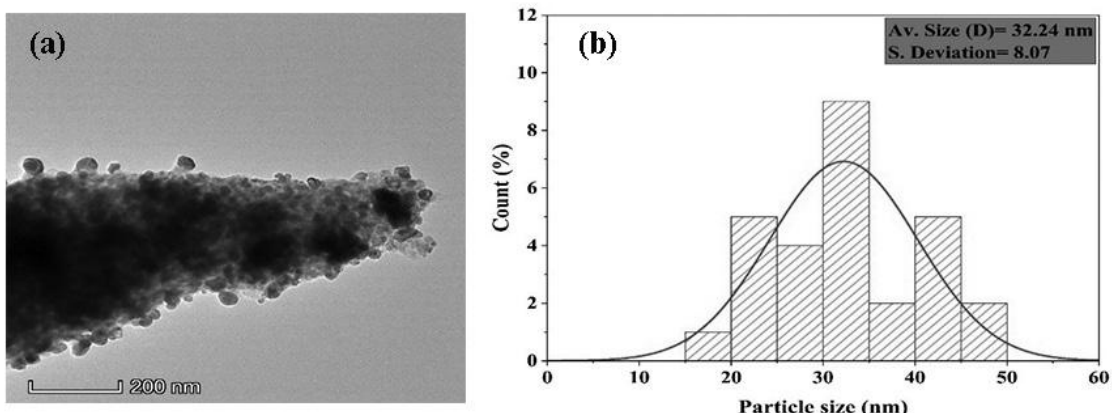


Fig. 7. TEM analysis of biosynthesized AgNPs mediated by *Bacillus siamensis* strain CCTB2. (a): TEM micrograph; (b) Size distribution plots).

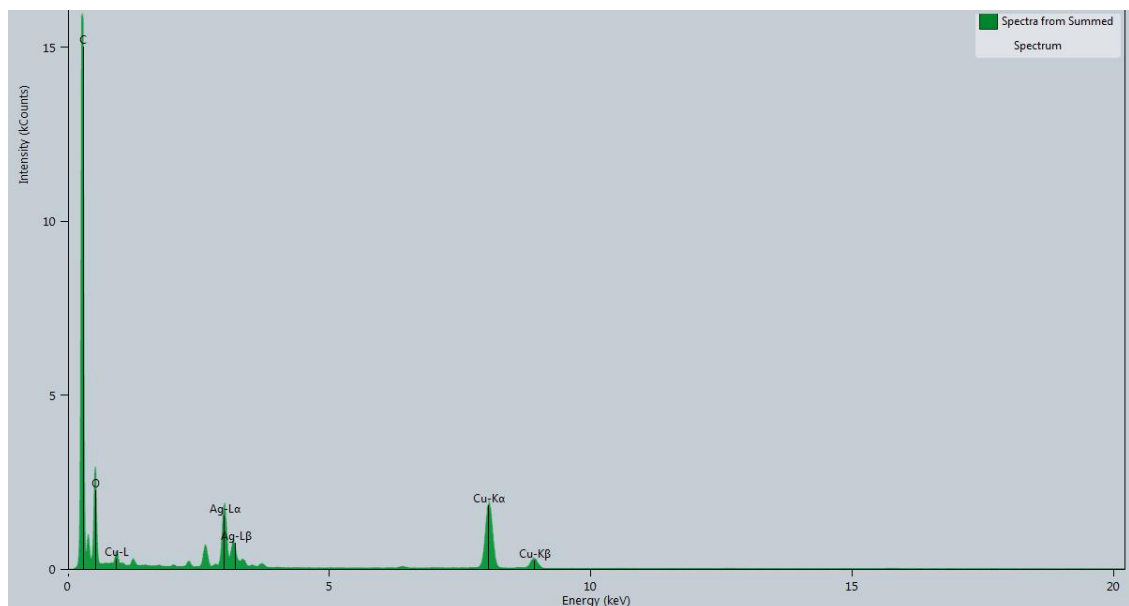


Fig. 8. EDS spectrum of biosynthesized AgNPs mediated by bacterial isolate CCTB2

mycelial growth increased with increasing their concentration. Silver nanoparticles (AgNPs) synthesized from the bacterial strain CCTB2 reduced mycelial diameter by 80.66%, 90.05%, and 96.65% as compared to

control plates at concentrations of 20, 30, and 40 μ g/mL, respectively (Fig. 9). The present study aligns with previous research that has shown the effectiveness of AgNPs as an antifungal agent in protecting plants against

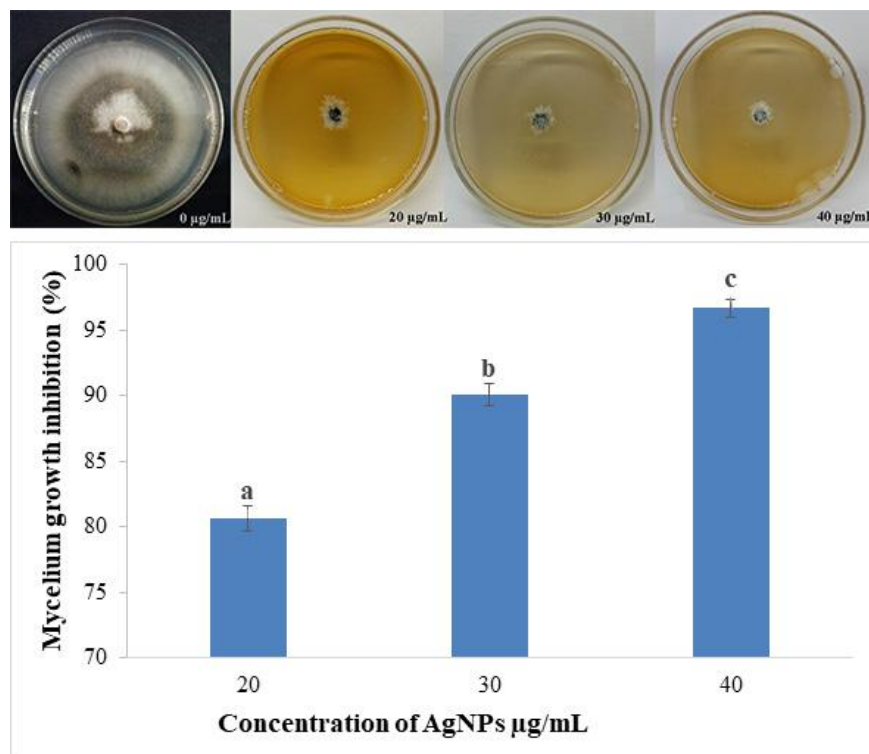


Fig. 9. Inhibition of mycelium growth of *Pyricularia oryzae* strain MP2 by *Bacillus siamensis* strain CCTB2 mediated AgNPs at different concentrations

fungal infections (Abd-Elsalam and Prasad, 2018; Masum *et al.*, 2019; Ibrahim *et al.*, 2020; Saha *et al.*, 2025).

Our results revealed that untreated hyphae maintained their typical structural features, including smooth surfaces, uniform branching, and robust, intact cell walls (Fig. 10). In contrast, exposure to AgNPs induced pronounced morphological alterations, evidenced by irregular and distorted hyphal growth, abnormal swelling at multiple regions, loss of structural integrity, and a markedly higher frequency of branching per unit hyphal length. These abnormalities

indicate that AgNPs disrupt normal hyphal development and compromise cell wall stability. Silver nanoparticles (AgNPs) show antifungal effects through multiple interrelated mechanisms, primarily by generating reactive oxygen species (ROS) and directly disrupting the cell membrane (Ibrahim *et al.*, 2020; Chandrakar *et al.*, 2025). These mechanisms often work together to cause significant cellular dysfunction, leading to the death of fungal cells. Additionally, microbial cell intrusion of AgNPs may cause damage to intracellular microorganelles (such as vacuoles and ribosomes) as well as biomolecules, including DNA, proteins, and

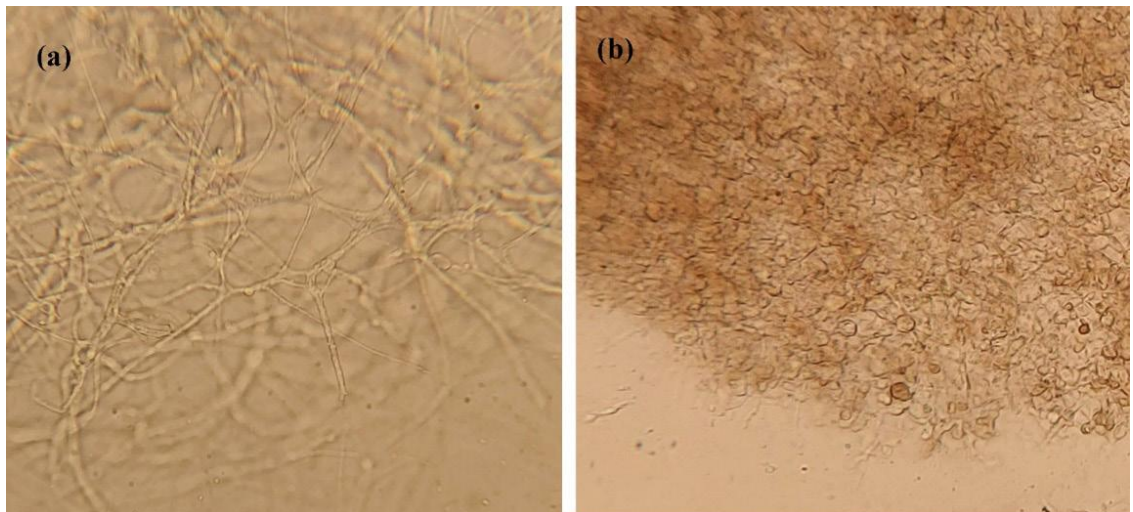


Fig. 10. Effect of AgNPs on the mycelial growth of *P. oryzae* strain SP2. (a) Uniform and intact hyphal structures observed in the control; (b) Aberrant structures, swelling, and cell wall damage in the presence of the biosynthesized AgNPs (40 µg/mL)

lipids (Dakal *et al.*, 2016). The modulation of intracellular signaling pathways may also lead to apoptosis (Lee and Jun, 2019).

Conclusion

The green synthesis of silver nanoparticles (AgNPs) is a safe alternative to physical and chemical methods. This study presents, for the first time, the production of AgNPs using a seaweed endophytic bacterium, *B. siamensis*. The formation of bio-synthesis AgNPs was further confirmed through UV-vis spectroscopy, FTIR, XRD, TEM, XRD, and EDX. Additionally, the biosynthesized silver nanoparticles demonstrated potent antifungal activity against the rice blast pathogen, *P. oryzae* strain MP2. The antimicrobial activity of AgNPs may be attributed to their ability to inhibit cell wall disintegration. In summary, the results indicate the potential

of biosynthesized AgNPs as an eco-friendly antifungal agent against blast disease. However, the greenhouse and field-level tests are necessary to verify their efficacy in semi-controlled and real agricultural situations and ensure reproducibility. The green synthesis strategy has high scale-up and commercialization potential, providing a sustainable alternative for agricultural system integration and long-term food security.

Acknowledgement

This research was financially supported by the Research Management Wing (Project No.: 003/2021-2024), Gazipur Agricultural University, Bangladesh.

Conflict of Interest

The authors affirm that no financial or commercial relationships that might be

construed as a potential conflict of interest existed during the course of the research.

Author Contributions

Chaiti Saha: Conceptualization, methodology, writing – original draft. Mst. Raihana Sultana: Methodology, Validation. Fahmida Khatun, Efat Tara Yesmean Riya & Nahid Hasan Saikat: Methodology, visualization and review of the manuscript. Abdul Kader & Md. Manjurul Haque: Validation, Resources. Md. Mahidul Islam Masum: Conceptualization, Methodology, Supervision, Funding acquisition, Writing – review & editing'. All the authors reviewed and endorsed the final manuscript.

References

Abd-Elsalam, K. A. and R. Prasad. 2018. Nanobiotechnology applications in plant protection. *Springer*

Asmaul, H., M. M. Asaduzzaman and N. M. I. M. Nor. 2021. Rice bakanae disease: an emerging threat to rice production in Bangladesh. *Asian J. Med. Biol. Res.* 6:608-10.

BBS. 2021. Yearbook of Agricultural Statistics of Bangladesh. p. 41: Statistics and Informatics Division (SID), Ministry of Planning, Government of the People's Republic of Bangladesh

Bhuiyan, M.S.H., A. Zahan, H. Khatun, M. Iqbal, F. Alam and M. R. Manir. 2014. Yield performance of newly developed test crossed hybrid rice variety. *Intl. J. Agron. Agril. Res.* 5: 48-54.

Bhuiyan, N. I., Paul, D. N. R. and Jabber, M. A. (2002). Feeding the extra millions by 2025 Challenges for rice research and extension in Bangladesh, National Workshop on Rice Research and Extension in Bangladesh, Bangladesh Rice Research Institute, Gazipur.

Boone, D. R., R. W. Castenholz and G. M. Garrity. 2001. Bergey's manual® of systematic bacteriology. *Springer Science & Business Media* 2nd Edn. Pp. 305-1106.

Chafidz, A., A. R. Afandi, B. M. Rosa, J. Suhartono, P. Hidayat and H. Junaedi. 2020. Production of silver nanoparticles via green method using banana raja peel extract as a reducing agent. *Com. Sci. Tech.* 5:112-18.

Chandrakar, N., S. K. Shukla, D. Karley, N. Upadhyay and Y. V. Nancharaiah. 2025. Biogenic Silver Nanoparticles Exhibit Antifungal and Antibiofilm Activity Against *Candida albicans* via Intracellular ROS Production. *APMIS*. 133:e70061.

Dada, A. O., J. Ojediran, F. Dada, A. Olalekan and O. Awakan. 2017. Green synthesis and characterization of silver nanoparticles using *Calotropis procera* extract. *J. Appl. Chem. Sci.* 8:137-43.

Darweesh, M. A., M. Y. Elgendi, M. I. Ayad, A. M. M. Ahmed, N. K.

Elsayed and W. Hammad. 2022. A unique, inexpensive, and abundantly available adsorbent: Composite of synthesized silver nanoparticles (AgNPs) and banana leaves powder (BLP). *Heliyon.* 8

Dean, R., J. A. Van Kan, Z. A. Pretorius, K. E. Hammond-Kosack, A. Di Pietro, P. D. Spanu, J. J. Rudd, M. Dickman, R. Kahmann, J. Ellis and G. D. Foster. 2012. The Top 10 fungal pathogens in molecular plant pathology. *Mol. Plant Pathol.* 13:414-30.

Fernandez, J. and K. Orth. 2018. Rise of a Cereal Killer: The Biology of *Magnaporthe oryzae* Biotrophic Growth. *Trends Microbiol.* 26:582-97.

Fouda, M. M. G., N. R. Abdelsalam, I. M. A. Gohar, A. E. M. Hanfy, S. I. Othman, A. F. Zaitoun, A. A. Allam, O. M. Morsy and M. El-Naggar. 2020. Utilization of High throughput microcrystalline cellulose decorated silver nanoparticles as an eco-nematicide on root-knot nematodes. *Colloids and Surfaces B: Biointerfaces.* 188:110805.

Gao, T., H. Zhou, W. Zhou, L. Hu, J. Chen and Z. J. M. Shi. 2016. The fungicidal activity of thymol against *Fusarium graminearum* via inducing lipid peroxidation and disrupting ergosterol biosynthesis. *Molecules,* 21:770.

Ghatak, A., L. Willocquet, S. Savary and J. Kumar. 2013. Variability in Aggressiveness of Rice Blast (*Magnaporthe oryzae*) Isolates Originating from Rice Leaves and Necks: A Case of Pathogen Specialization? *PLOS ONE.* 8:e66180.

Hari, S. B., P. S. Briste, A. A. Sumi, M. K. Mosharaf, S. I. Paul, M. M. I. Masum and R. Jannat. 2023. Endophytic bacteria isolated from medicinal plants induce plant growth promotion and southern blight disease suppression in tomato. *J. Plant Pathol.* 105:197-210.

Hossain, A., J. Luo, M. A. Ali, R. Chai, M. Shahid, T. Ahmed, M. M. Hassan, R. H. Kadi, Q. An and B. Li. 2023. Synergistic Action of Biosynthesized Silver Nanoparticles and Culture Supernatant of *Bacillus amyloliquefacience* against the Soft Rot Pathogen *Dickeya dadantii*. *Plants.* 12:1817.

Hossain, M., M.A. Ali, and M. D. Hossain. 2017. Occurrence of blast disease in rice in Bangladesh. *J. Agric. Biol. Sci.* 4:74-80.

Huq, M. A. 2020. Green synthesis of silver nanoparticles using *Pseudoduganella eburnea* MAHUQ-39 and their antimicrobial mechanisms investigation against drug resistant human pathogens. *Int. J. Mol. Sci.* 21:1510.

Ibrahim, E., J. Luo, T. Ahmed, W. Wu, C. Yan and B. Li. 2020. Biosynthesis

of Silver Nanoparticles Using Onion Endophytic Bacterium and Its Antifungal Activity against Rice Pathogen *Magnaporthe oryzae*. *J. Fungi*. 6:294.

Joseph, J., H. Sasidharan and O. J. I. J. S. R. i. B. S. V. Chithira. 2018. Isolation, production and characterisation of novel gelatinase enzyme from *Bacillus* spp. *Int. J. Sci. Res. Biol. Sci.* 5:6.

Juhmani, A.-S., A. Vezzi, M. Wahsha, A. Buosi, F. D. Pascale, R. Schiavon and A. Sfriso. 2020. Diversity and Dynamics of Seaweed Associated Microbial Communities Inhabiting the Lagoon of Venice. *Microorganisms*. 8:1657.

Jyoti, K., M. Baunthiyal and A. Singh. 2016. Characterization of silver nanoparticles synthesized using *Urtica dioica* Linn. leaves and their synergistic effects with antibiotics. *J. Radiat. Res. Appl. Sci.* . 9:217-27.

Khan, M. A. I., M. A. Ali, M. A. Monsur, A. Kawasaki-Tanaka, N. Hayashi, S. Yanagihara, M. Obara, M. A. T. Mia, M. A. Latif and Y. Fukuta. 2016. Diversity and Distribution of Rice Blast (*Pyricularia oryzae* Cavara) Races in Bangladesh. *Plant Disease*. 100:2025-33.

Kumar, M. and S. Ashraf. 2019. Effect of bioagents on the growth of rice against blast disease caused by *Pyricularia oryzae*. *J. Pharmacogn. Phytochem*. 8:84-88.

Lee, S. H. and B.-H. Jun. 2019. Silver nanoparticles: synthesis and application for nanomedicine. *Int. J. Sci. Res. Biol. Sci.* 20:865.

Liu, J. and R. H. Hurt. 2010. Ion release kinetics and particle persistence in aqueous nano-silver colloids. *Environ. Sci. Technol.* 44:2169-75.

Mahajan, M., P. Jethwani, C. Mootapally, I. Pancha, R. P. Singh and N. Nathani. 2025. Seaweed-Bacteria Interaction, Molecular Mechanism and Biotechnological Applications. In *Biotechnological Interventions to Aid Commercial Seaweed Farming*, ed. MS Rathore, VA Mantri:393-424. Singapore: Springer Nature Singapore.

Manikandan, R., M. Beulaja, R. Thiagarajan, S. Palanisamy, G. Goutham, A. Koodalingam, N. Prabhu, E. Kannapiran, M. J. Basu and C. Arulvasu. 2017. Biosynthesis of silver nanoparticles using aqueous extract of *Phyllanthus acidus* L. fruits and characterization of its anti-inflammatory effect against H_2O_2 exposed rat peritoneal macrophages. *Proc. Biochem.* 55:172-81.

Masum, M., L. Liu, M. Yang, M. Hossain, M. Siddiq, M. Supty, S. Ogunyemi, A. Hossain, Q. An and B. Li. 2018. Halotolerant bacteria belonging to operational group *Bacillus amyloliquefaciens* in biocontrol of the rice brown stripe pathogen

Acidovorax oryzae. *J. Appl. Microbiol.* 125:1852-67.

Masum, M. M. I., M. M. Siddiqua, K. A. Ali, Y. Zhang, Y. Abdallah, E. Ibrahim, W. Qiu, C. Yan and B. Li. 2019. Biogenic synthesis of silver nanoparticles using *Phyllanthus emblica* fruit extract and its inhibitory action against the pathogen *Acidovorax oryzae* strain RS-2 of rice bacterial brown stripe. *Front. Microbiol.* 10:820.

Miah, G., M. Y. Rafii, M. R. Ismail, A. B. Puteh, H. A. Rahim, R. Asfaliza and M. A. Latif. 2013. Blast resistance in rice: a review of conventional breeding to molecular approaches. *Mol. Biol. Rep.* 40:2369-88.

Nasruddin, A. and N. Amin. 2013. Effects of cultivar, planting period, and fungicide usage on rice blast infection levels and crop yield. *J. Agril. Sci.* 5:160.

Raghu, S., M. K., Yadav, S.R. Prabhukarthikeyan, M. S. Baite, S. Lenka and M. Jena. 2018. Occurrence, pathogenicity, characterization of *Fusarium fujikuroi* causing rice bakanae disease from Odisha and in vitro management. *ORYZA: An International Journal of Rice*. 55:214-223.

Rajashekhar, M., E. Shahana and K. J. J. E. Z. S. Vinay. 2017. Biochemical and molecular characterization of *Bacillus* spp. isolated from insects. *J. Entomol. Zool. Stud.* 5:581-88.

Razu, M. A. U. and I. Hossain. 2015) Eco-friendly management of rice diseases. *Int. J. Appl. Sci. Biotechnol.* 3: 80-88.

Saha, C., S. Pandit, M. M. Hossain, M. M. Haque, R. Jannat, M. T. Rubayet and M. M. I. Masum. 2025. Eco-friendly biosynthesis of silver nanoparticles from banana flower extract for protective role against the rice blast pathogen *Pyricularia oryzae*. *Mater. Res. Express.* 12:095003.

Sarode, C., S. Bramhankar, S. Kakad, A. Labhasetwar, S. Bhure, S. Isokar and D. J. I. J. C. S. Tathod. 2019. Biochemical and physiological characterizations of *Bacillus subtilis*. 7:1957-60.

Sella, L., V. V. Vu, A. Quarantin, R. Caracciolo, R. Govind, A. Bolzonello, S. Tundo, M. De Zotti, F. Favaron, H. D. Nguyen, Q. L. Le, T. T. Nguyen, L. T. Do and H. M. Nguyen. 2021. Sustainable Methods to Control *Pyricularia oryzae*, the Causal Agent of Rice Blast Disease. In *Innovations in Land, Water and Energy for Vietnam's Sustainable Development*, ed. M Anderle:67-82. Cham: Springer International Publishing.

Shang, Y., M. K. Hasan, G. J. Ahammed, M. Li, H. Yin and J. Zhou. 2019. Applications of Nanotechnology in Plant Growth and Crop Protection: A Review. *Molecules*. 24:2558.

Singh, P., H. Singh, Y. J. Kim, R. Mathiyalagan, C. Wang and D. C.

Yang. 2016. Extracellular synthesis of silver and gold nanoparticles by *Sporosarcina koreensis* DC4 and their biological applications. *Enzyme Microb. Technol.* 86:75-83.

Suji, H. A., K. Manikandan, A. Sudha, A. Muthukumar, C. Jeyalakshmi, M. Charumathi, M. Rajesh and T. S. Raj. 2024. Whole genome sequence of seaweed endophyte *Bacillus halotolerans* strain AUPP for antagonistic activity against *Fusarium incarnatum* causing chilli fruit rot. *Sci. Rep.* 14:31881.

Sun, Q., X. Cai, J. Li, M. Zheng, Z. Chen and C.-P. Yu. 2014. Green synthesis of silver nanoparticles using tea leaf extract and evaluation of their stability and antibacterial activity. *Colloids Surf. A Physicochem. Eng. Asp.* 444:226-31.

Tiwari, H., K. Samal, S. R. Geed, S. Bera, C. Das and K. Mohanty. 2023. Green synthesis of silver nanoparticles for ultrafiltration membrane surface modification and antimicrobial activity. *Sust. Chem. Clim. Act.* 3:100031.

Wilson, R.A. and N.J. Talbot. 2009. Under pressure: investigating the biology of plant infection by *Magnaporthe oryzae*. *Nature Rev. Microbiol.* 7: 185-195.